Joint and muscle-tendon coordination strategies during submaximal jumping

Logan Wade[1]

Glen A Lichtwark[1]

Dominic J Farris[1, 2]

[1] School of Human Movement and Nutrition Sciences, The University of Queensland, Brisbane, Australia

[2] Sport and Health Sciences, University of Exeter, Exeter, UK

All authors contributed substantially to concept design, experimental design, and data analysis. Logan Wade performed all data collection, data processing and writing. Glen Lichtwark and Dominic Farris both contributed substantially to manuscript revision.

Running Head: Joint and muscle coordination strategies during jumping

Keywords: fascicle, ultrasound, EMG, muscle coordination, biomechanics

Corresponding Author:

Logan Wade

1 West, Office 5.113,

Bath, BA2 7AY, United Kingdom

lw2175@bath.ac.uk

Abstract

Previous research has demonstrated that during submaximal jumping, humans prioritize reducing energy consumption by minimizing countermovement depth. However, sometimes movement is constrained to a non-preferred pattern and this requires adaptation of neural control that accounts for complex interactions between muscle architecture, muscle properties, and task demands. This study compared submaximal jumping with either a preferred or deep countermovement depth to examine how joint and muscle mechanics are integrated into the adaptation of coordination strategies in the deep condition. Three-dimensional motion capture, two force plates, electromyography and ultrasonography were used to examine changes in joint kinetics and kinematics, muscle activation and muscle kinematics for the lateral gastrocnemius and soleus. Results demonstrated that a decrease in ankle joint work during the deep countermovement depth was due to increased knee flexion, leading to unfavorably short bi-articular muscle lengths and reduced active fascicle length change during ankle plantar flexion. Therefore, ankle joint work was likely decreased due to reduced active fascicle length change and operating position on the force-length relationship. Hip joint work was significantly increased as a result of altered muscle activation strategies, likely due to a substantially greater hip extensor muscle activation period compared to plantar flexor muscles during jumping. Therefore, coordination strategies at individual joints are likely influenced by time availability, where a short plantar flexor activation time results in dependence on muscle properties, instead of simply altering muscle activation, while the longer time for contraction of muscles at the hip allows for adjustments to voluntary neural control.

New and Noteworthy

Using human jumping as a model, we show that adapting movement patterns to altered task demands is achieved differently by different muscles across the leg. In muscles with reduced activation periods due to proximal-to-distal sequencing (i.e. plantar flexors), muscle contractile properties (force-length relationship) are relied on to adapt joint kinetics, while voluntary activation is adapted in muscles with greater activation periods, such as the hip extensors.

Introduction

Whole-body movement typically requires the coordination of numerous joints and muscles in order to perform the desired action. Studies examining how preferred human movement is coordinated have demonstrated that a high priority is placed on strategies that minimize energy consumption (8, 13, 29, 35, 38, 54). However, human movement is not always performed under ideal conditions where preferred joint mechanical coordination strategies may be achieved. Instead, joint coordination strategies must be adapted to numerous constraints that exist during everyday life. Jumping is an ideal task to examine preferred joint coordination strategies because it is a full body movement that can be easily manipulated and constrained. Vanrenterghem et al. (54) demonstrated that during submaximal jumping, preferred movement patterns minimize energy consumption by decreasing countermovement depth (CMD), decreasing reliance on segments with large inertia, and increasing contributions of ankle plantar flexor muscles and elastic structures (52, 54). Such evidence suggests that we optimize our CMD to suit the jump height required. However, a simulation study of squat jumping has suggested that a deeper CMD than preferred could potentially increase jump height in a maximal jumping task (12). This result has not been found in experimental studies (12, 34), but it is unclear why, and what factors are influencing our preferred movement choice in this case.

When jumping to submaximal heights, power output is not maximized, and more options for generating the required power are available. Submaximal jumping with a deep countermovement necessitates a greater work contribution about the knee and hip, compared to our preference for performing submaximal work about the ankle (54). This presents an interesting constrained task, where ankle muscle work might be restricted so as to not overshoot the jump height target. Alternatively, the coordination strategies across all lower limb joints might be altered to reduce work, although altering the muscle activation across all lower limb joints, as opposed to just across the ankle, might result in an inconsistent jump height and may be less likely to be employed. Restricted ankle work could be performed through inherent changes in muscle contractile mechanics, or changes in activation by the nervous system. It has been suggested that the force-velocity (24) and force-length properties (18) of muscle may provide an inherent stability to maintain

78 movement coordination despite perturbations during explosive movements such as jumping (26, 49).
79 Simulation studies have found that without muscle properties, a jumping model was unable to recover from
80 a perturbation compared to a Hill-type muscle model, which was only slightly affected (49). A follow up
81 study found that the force-length or force velocity relationship corrected for different perturbations, with
82 the force-length relationship providing good resistance to static perturbations and the force-velocity
83 relationship providing good resistance to dynamic perturbations (17). Muscle contractile mechanics
84 therefore allow joint coordination to be adapted at the instant the perturbation is applied, correcting the
85 action to complete the task without changes to neural control. Simulations examining maximal vertical
86 squat jump height from a range of static starting squat depths indicate that changes in muscle contractile
87 properties counteracted perturbations to such a degree that a single stimulation pattern could be applied
88 for all starting positions to achieve the vertical jump (50). A human experimental study challenged this,
89 identifying that the onset of muscle activations in the ankle plantar flexors were significantly delayed as
90 squat depth increased, with simulations determining this a requirement to optimize jump height (5).
91 Therefore, performing maximal jumping from altered countermovement depths will likely require changes
92 in both muscle activation strategies and muscle contractile mechanics. This may be further complicated
93 because of the complex muscle-tendon interactions that occur in ankle plantar flexor muscles during
94 jumping (30).

95

96 Humans store energy in the Achilles tendon against the resistance of bodyweight during squat jumping,
97 thus energy is stored at the bottom of the squat prior to push-off (15). A high proportion of ankle joint
98 work during jumping is delivered via elastic recoil of the Achilles tendon as muscle force decreases to near
99 zero prior to take-off (30, 31). Because work from the Achilles tendon recoil comes at low cost, this results
100 in a reliance on ankle joint work, in preference to the hip or knee, during push-off for submaximal jumping
101 (54, 55). However, a deep countermovement will require work to be performed proximally in the limb (54),
102 therefore the energy that is stored in the Achilles tendon could lead to potential excess energy for the
103 jumping movement. ~~If joint coordination patterns are not altered to dissipate that excess energy, the jump~~
104 ~~might overshoot the submaximal target height~~. Limiting ankle joint work to avoid overshoot may be
105 accomplished by changes in muscle activation or potentially by altered operating position on the force-

length or force-velocity relationship, especially in bi-articular muscles (17, 48, 49, 56). If ankle joint work is not limited sufficiently by changes in muscle contractile mechanics or muscle activation strategies, too much energy may be stored in the tendon which may then need to be reabsorbed back into the muscle. This mechanism, termed tendon 'backfire', has been found in frog muscle and simulation studies (3, 43), although such a mechanism has not been demonstrated during human movement. Backfire is undesirable and occurs when energy that is stored in the tendon by active muscle fascicle shortening, is then reabsorbed by active fascicle lengthening (3, 43), either when the muscle-tendon unit is isometric or shortening. In the dynamic jumping movement, backfire would therefore be exhibited in the form of fascicle lengthening while the muscle-tendon unit shortens. During energy dissipation tasks such as landing, significant energy is stored in tendons that must be reabsorbed by the muscle (44, 57), therefore there is potential for backfire to exist in humans, although this would be an undesirably inefficient solution. It is therefore interesting to study how humans adjust ankle plantar flexor muscle function to adapt to a deeper than preferred countermovement during submaximal jumping, as a potential scenario in which the backfire phenomenon might be observed.

The aim of this study was to examine how muscle contractile mechanics and activation are altered to overcome a constrained task, whereby participants are required to perform a sub-maximal jump with either a deep or preferred CMD. It was hypothesized that during submaximal jumping with a deep CMD, energy stored in the Achilles tendon by resisting body weight at the bottom of the squat would be reabsorbed (backfire) by the plantar flexor muscle fascicles to avoid overshooting the target jump height.

Methods

Twelve male participants (age = 25.4 ± 3.6 years, height = 1.79 ± 0.05 m, mass = 80.3 ± 3.6 kg) gave written informed consent to participant in this study with ethics approved by the institutional ethics review committee at the University of Queensland (Approval number: HMS15/1106). Both males and females were recruited for this study, however due to participant availability, only males were able to be included.

Prior to data collection, participants performed maximal countermovement jumps in order to determine the required deep CMD and submaximal jump height. During experimental data collection, participants performed barefoot submaximal countermovement jumps at a preferred or deep CMD without arm swing. Countermovement depth was defined as the vertical displacement of the COM between standing and the bottom of the countermovement (see below for calculation). During testing, the deep CMD was set as 130% of the self-selected CMD during maximal countermovement jumping (determined prior to experimental data collection). Submaximal jump height was set to 60% of maximal jump height. Submaximal jump height and CMD were calculated live from ground reaction force (GRF) data using the double integration method (28, 53). Submaximal jumps were deemed successful if jump height and CMD (deep CMD only) were within 2 cm of the target jump height and CMD (deep CMD only). Participants had a light-box installed in front of their jumping platform that consisted of a horizontal row of LED lights located behind a double slit, ensuring the light could only be seen when participant's eyes were horizontal to the light-box at the apex of the jump. Live calculation of jump height and CMD (deep CMD only) were used to provide verbal feedback to participants after each trial. During the deep CMD, a rope was suspended behind the participant so that it could be felt along the back of the thighs at the correct CMD. All jumps were recorded but only successful jumps were used in data analysis. If a jump was not deemed successful, the condition was repeated until 3 successful jumps were recorded, or the participant had performed a total of 10 jumps. Participants were given 30 seconds of rest between each jump. Participants were given an unweighted weight vest that was worn during testing with instructions to lock their hand onto the vest to ensure that they did not use their arms during jumping.

Kinetics and Kinematics

GRF data were collected from two force plates (one foot on each plate) located within an instrumented treadmill (Instrumented Tandem Treadmill, AMTI, MA, USA). Using LabVIEW (National Instruments Corporation, Austin, USA), GRF data were sampled at 2000Hz via AMTI force plate amplifiers (AMTI Gen 5, AMTI, MA, USA) and recorded using LabVIEW at 1000Hz (down-sampled due to LabVIEW sampling limitations). Vertical GRF's from each plate were summed and a custom script calculated jump

159 height and countermovement depth live, using the double integration method outlined by Vanrenterghem
160 et al. (53). Countermovement depth was identified as the displacement of the COM from standing to the
161 bottom of the countermovement, considered to be when the center of mass velocity was equal to zero (53).
162 Force data for full analysis was simultaneously recorded using Qualisys Track Manager software (Qualisys,
163 Gothenburg, Sweden) via AMTI force plate amplifiers at 2000 Hz. Vertical GRF's from each plate were
164 summed and then during two seconds of quiet standing prior to jumping, vertical GRF data were averaged
165 to calculate the weight of the participant, which was subtracted from the vertical GRF to calculate net GRF.
166 Net GRF maximum, minimum and standard deviation (STD) were identified during quiet standing and
167 then these values were used to identify the first time point where the moving average of net GRF (50 ms
168 window) deviated by more than the maximum or minimum range ± the STD. From this time point, net
169 GRF data were then tracked in reverse to find the first instance after net GRF was zero and identified this
170 point as the start of the movement. End of the movement (take-off) was defined as the point at which the
171 net GRF was equal to negative participant weight. Post-hoc offline calculation of jump height employed a
172 modified version of a hybrid method outlined by Aragón-Vargas (2), whereby net GRF was divided by
173 body mass to calculate COM acceleration, and then COM acceleration was integrated to calculate COM
174 take-off velocity. Take-off velocity was then combined with projectile motion equation to calculate flight
175 distance (see Aragón-Vargas (2) for in-depth details using the projectile motion equation). Heel lift, defined
176 as the displacement of the center of mass between quiet standing and take-off, was calculated by measuring
177 the average vertical displacement of the left and right anterior superior iliac spine (ASIS) and posterior
178 superior iliac spine (PSIS) markers between standing and take-off. Distance travelled in the air and heel lift
179 were summed to calculate jump height. This reduces errors that may be introduced by double integration
180 amplifying small errors in the data over time, which has a greater effect on the deep CMD as it takes longer
181 to perform.

182

183 An eight camera, three-dimensional (3D) optoelectronic camera system (Oqus, Qualisys, AB, Sweden) was
184 used to capture kinematic data (200 Hz) during jumping. Reflective markers were placed on the body at the
185 left and right acromion processes, C7 vertebrae, suprasternal notch of the manubrium, ASIS, PSIS and on
186 the left and right iliac crest directly superior to the greater trochanter. Markers were placed on the medial

and lateral joint center of rotation of the knee, medial and lateral malleolus of the ankle, posterior aspect of the calcaneus, first and fifth metatarsal-phalangeal joints and the end of the distal phalanx of the first toe. Thigh and shank four-marker clusters were placed midway between joints using Velcro strapping. Markers were labelled for each trial and kinematic and kinetic data were exported to OpenSim (11). A generic model (20) was modified to remove the arms and hands with their masses added to the trunk, and the cervical joint between the trunk and the head was locked. The model was scaled to the dimensions of the participant using quiet standing static calibration trials with distribution of segment masses kept the same as the generic model. Inverse kinematics were then performed in OpenSim using a weighted least-squares fit of the model markers to the experimental markers during jumping trials. During processing, inverse kinematic marker positions and inverse dynamics forces were low-pass filtered at 25 Hz using a second order two-way Butterworth filter. Joint moments were calculated using an inverse dynamics solution and then both inverse kinematics and dynamics results were exported to MATLAB (Mathworks, MA, USA) for further analysis. In MATLAB, joint angles from inverse kinematics were differentiated using the central difference technique to calculate joint angular velocities and multiplied by joint moments to calculate joint powers (ankle, knee and hip) in both legs. Left and right joint powers for the hip, knee and ankle were summed and then trimmed from the start of the countermovement phase until take off from GRF data outlined previously. Finally, joint powers were integrated to find net work about each joint from the start of the countermovement until take-off. Relative joint contributions to total net work were identified by dividing the individual net work of each joint by the summed net work of the hip, knee and ankle joints.

Electromyography (EMG)

EMG data were collected unilaterally on the right leg from the soleus (SOL), lateral gastrocnemius (LG), vastus lateralis (VL), rectus femoris (RFEM), biceps femoris (BFEM), and gluteus maximus (GMAX) using a wireless EMG system (MYON m320, MYON, Schwarzenberg, Switzerland). Bipolar EMG electrodes were placed over the belly of each muscle according to the SENIAM guidelines (21). Raw EMG data were recorded in Qualisys Track Manager at 2000 Hz. EMG signals were bandpass filtered (30-350 Hz), rectified and averaged using a rolling root-mean-squared (RMS) calculation over windows of 100 consecutive frames

(50 ms). Substantial muscle activation was defined as the point where EMG activation sharply increased and spiked during ankle plantar flexion. Onset of substantial muscle activation was manually identified in a blinded fashion (25), and EMG was normalized against the mean values recorded in the preferred CMD condition during the period of substantial muscle activation. Maximal normalized EMG amplitude was identified by finding the maximal normalized EMG value between the start of substantial muscle activation until take-off (25). Integrated normalized EMG was calculated by performing trapezoidal integration from the start of substantial muscle activation until take-off, therefore the units for this measure are %Mean activation.seconds (%Ma.s). This measure represents a combination of how long the muscle was activated for and the level of muscle activation.

Muscle mechanics

Using OpenSim (11), muscle-tendon unit (MTU) lengths of the LG and SOL throughout the jumping movement were measured based on models of each muscle included within the rigid-body model (20). Muscle fascicles were imaged using a 96 element flathead ultrasound transducer (LZ 7.5/60/96Z, Telemed, Lithuania) placed over the LG and SOL muscle bellies, enabling imaging of both muscles (as per Farris and Raiteri, 2017). Using ultrasound gel applied to the transducer's surface, a suitable image location was found where both the LG and SOL were aligned. Participants were then asked to perform and hold a heel raise to determine if the probe alignment was sufficient to image fascicle shortening throughout the movement. The probe was then fixed to the participant using a self-adhesive bandage (Medichill, WA, Australia). Ultrasound images were recorded at 80 Hz and fascicle lengths were tracked using UltraTrack software (14). Manual corrections were made when the automated tracking algorithm did not sufficiently track the fascicles, however the researcher tracking the fascicles was blind to the conditions so as not to introduce bias. Statistical analysis was performed over sections of MTU and fascicle length change, based on timing of maximal fascicle length and start of substantial muscle activation. Start of muscle fascicle shortening was identified by finding the instant of maximum fascicle length for each trial. Onset of active fascicle shortening (AFS) was identified as either the point where the muscle began to shorten (post maximal fascicle length) or the start of substantial muscle activation, whichever occurred last.

Data reduction and statistical analysis

Due to quality of the image, ultrasound data of two participants for LG and one participant for SOL were excluded. Due to equipment dropout, EMG data of RFEM and BFEM are missing for one participant. Statistical analysis was performed in GraphPad Prism 7 software (GraphPad Software Inc, California, USA) by first performing D'Agostino and Pearson normality tests. If normality tests were passed then a paired t-test was performed comparing outcome measures between the deep CMD and the preferred CMD for total net work, jump height, integrated EMG and maximal EMG of all six muscle; as well as fascicle lengths, MTU length and timing offset between substantial muscle activation and maximum fascicle length for the SOL and LG. If normality tests were not passed, then a Wilcoxon matched-pairs signed rank test was used. Comparisons of net work, maximal moment and range of motion about the hip, knee and ankle joints were performed using 2 x 3 (condition x joint) two-way repeat measures ANOVA. If a main or interaction effect was found then post hoc analyses were performed to examine differences between each joint in the deep or preferred CMD conditions Multiple comparison corrections for t-tests and ANOVA post hoc analysis were performed using a Benjamini and Hochberg false discovery rate (5%) approach. This reduced the alpha value threshold from 0.05 to 0.0284. All P-values are reported but only P-values that fell below the adjusted threshold were considered significant. 95% confidence intervals are reported for all comparisons. All dispersion measures stated in text are STD.

Results

There was no significant difference in total net work (P = 0.405, CI -0.09 to 0.20 J/kg, Figure 1) and jump height (deep = 0.306 ± 0.046 m, preferred = 0.298 ± 0.050 m, P = 0.230, CI -0.006 to 0.024 m) between the deep or preferred CMD conditions and therefore individual net work contributions about each joint may be compared directly.

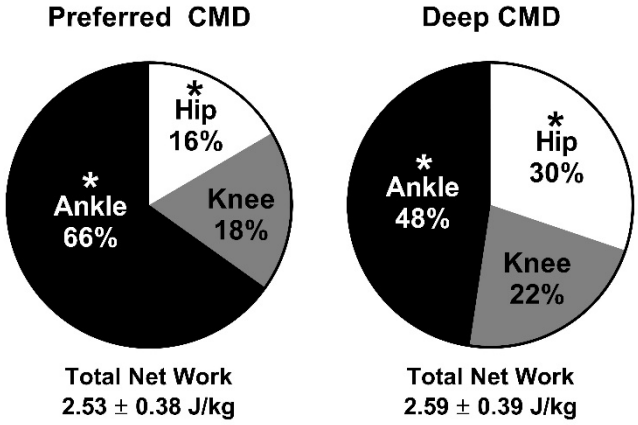

Figure 1: Net work about the hip (white), knee (grey) and ankle (black) joints during the preferred and deep countermovement depth conditions. * indicates a significant difference compared to the same joint in the alternate condition. Joint work was compared using a two-way repeat measures ANOVA (N = 12).

Joint mechanics

In the deep CMD condition, net work (Figure 1) increased about the hip joint by 0.363 ± 0.167 J/kg (P < 0.001, CI 0.230 to 0.495 J/kg), did not significantly increase about the knee by 0.112 ± 0.219 J/kg (P = 0.096, CI -0.021 to 0.244 J/kg), and significantly decreased about the ankle joint by 0.417 ± 0.254 J/kg (P < 0.001, CI -0.549 to -0.284 J/kg). Hip range of motion from minimum angle until take-off was 25.6 ± 11.7° greater in the deep CMD than in the preferred CMD (P < 0.001, CI 20.1 to 31.1°, Figure 2A), knee range of motion was 28.2 ± 10.6° greater in the deep CMD than preferred CMD (P < 0.001, CI 22.7 to 33.7°, Figure 2B) and ankle range of motion was not significantly different between conditions (P = 0.527, CI -7.2 to -3.8°, Figure 2C). Maximal hip moment during the deep CMD was 28.6 ± 21.2 Nm greater than preferred CMD (P < 0.001, CI 14.7 to 42.4 Nm, Figure 2D), maximal knee moment remained constant (P = 0.512, CI -9.4 to 18.4 Nm, Figure 2E) and maximal ankle moment was 33. 7 ± 16.6 Nm less in the deep CMD than preferred CMD (P < 0.001, CI -19.8 to -47.6 Nm, Figure 2F). Thus, the increase in work about

284 the hip was due to an increase in hip moment and range of motion while the decrease in ankle work was
285 due to a decrease in moment alone, as range of motion did not change.

286

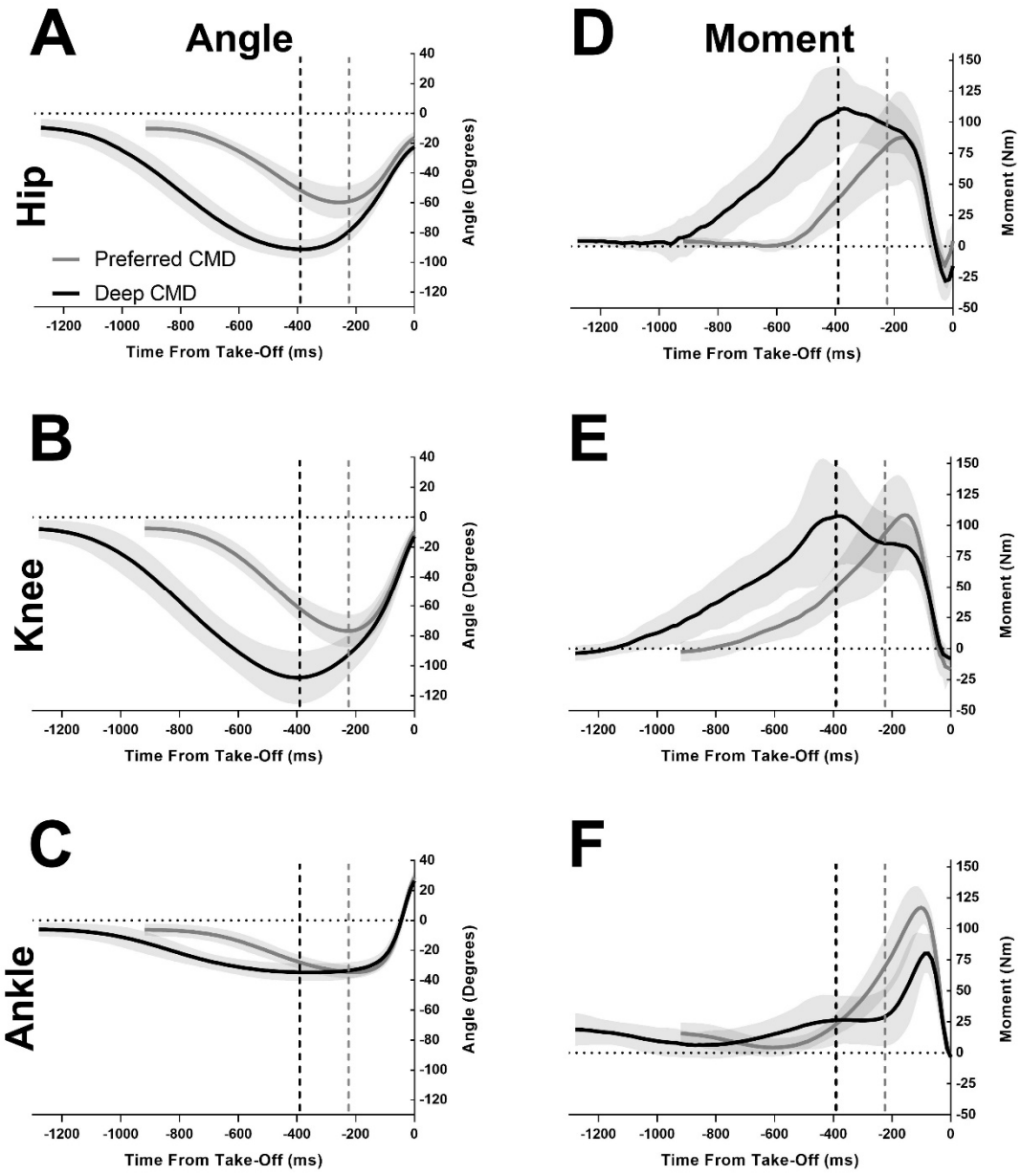

Figure 2: Mean (± STD) joint angles (A, B and C) and moments (D, E and F) about the hip (A and D), knee (B and E) and ankle (C and F) during the preferred CMD (Grey) and the deep CMD (Black). Vertical lines indication bottom of the countermovement. Joint range of motion and peak moment were analysed (N = 12) using a two-way repeat measures ANOVA.

287

288

289

Muscle

Compared to preferred CMD, integrated EMG (Figure 3A-3F) in the deep CMD was significantly higher for the GMAX (0.96 ± 1.00, CI 0.32 to 1.60, P = 0.007), BFEM (0.39 ± 0.21, CI 0.25 to 0.53, P < 0.001), RFEM (0.42 ± 0.47, CI 0.11 to 0.74, P = 0.005), VL (0.39 ± 0.27, CI 0.22 to 0.57, P < 0.001), lower for the LG (-0.08 ± 0.09, CI -0.14 to -0.03, P = 0.008) and did not change significantly in the SOL (CI -0.11 to 0.01, P = 0.058). Maximal EMG (Figure 3A-3F) was significantly different only in the GMAX, 1.14 ± 1.19 higher in the deep than preferred CMD (CI 0.39 to 1.89, P = 0.007).

In both conditions, the LG and SOL fascicles lengthened during the initial descending portion of countermovement by 8-9 ± 4 mm and 16 ± 5 mm respectively, from start of the movement until maximal fascicle length, with no difference between conditions (CI = LG -2.6 to 3.7 mm & SOL -0.4 to 2.4 mm, P > 0.143). In the preferred CMD, onset of substantial muscle activation coincided with maximal fascicle length for the LG (P = 0.827, CI -50 to 41 ms, Figure 3F) and occurred prior to maximal fascicle length in the SOL (P = 0.003, CI -80 to -22 ms, Figures 3E). In the deep CMD, onset of substantial muscle activation was significantly later than the occurrence of maximal fascicle length for both muscles (CI = LG 207 to 563 ms & SOL 181 to 419 ms, P < 0.003). AFS was significantly reduced in the deep CMD by 10 ± 10 mm in the LG (CI 3 to 17 mm, P = 0.011) and 4 ± 5 mm in the SOL (CI 1 to 8 mm, P = 0.0278) compared to the preferred CMD (Figure 3I and 3J). MTU lengths of the LG in the deep CMD condition shortened significantly more during the initial countermovement phase (3 ± 4 mm, CI 1 to 6 mm, P = 0.018) and as such, LG MTU lengths shortened significantly less during AFS (7 ± 2 mm, CI -5 to -9 mm, P < 0.001, Figure 3G). SOL MTU lengths did not change between conditions across any phase which is likely due to no change in ankle angle between the CMD conditions (P > 0.231, CI = Initial -2 to 2 mm & AFS = -3 to 1 mm, Figure 3H).

315

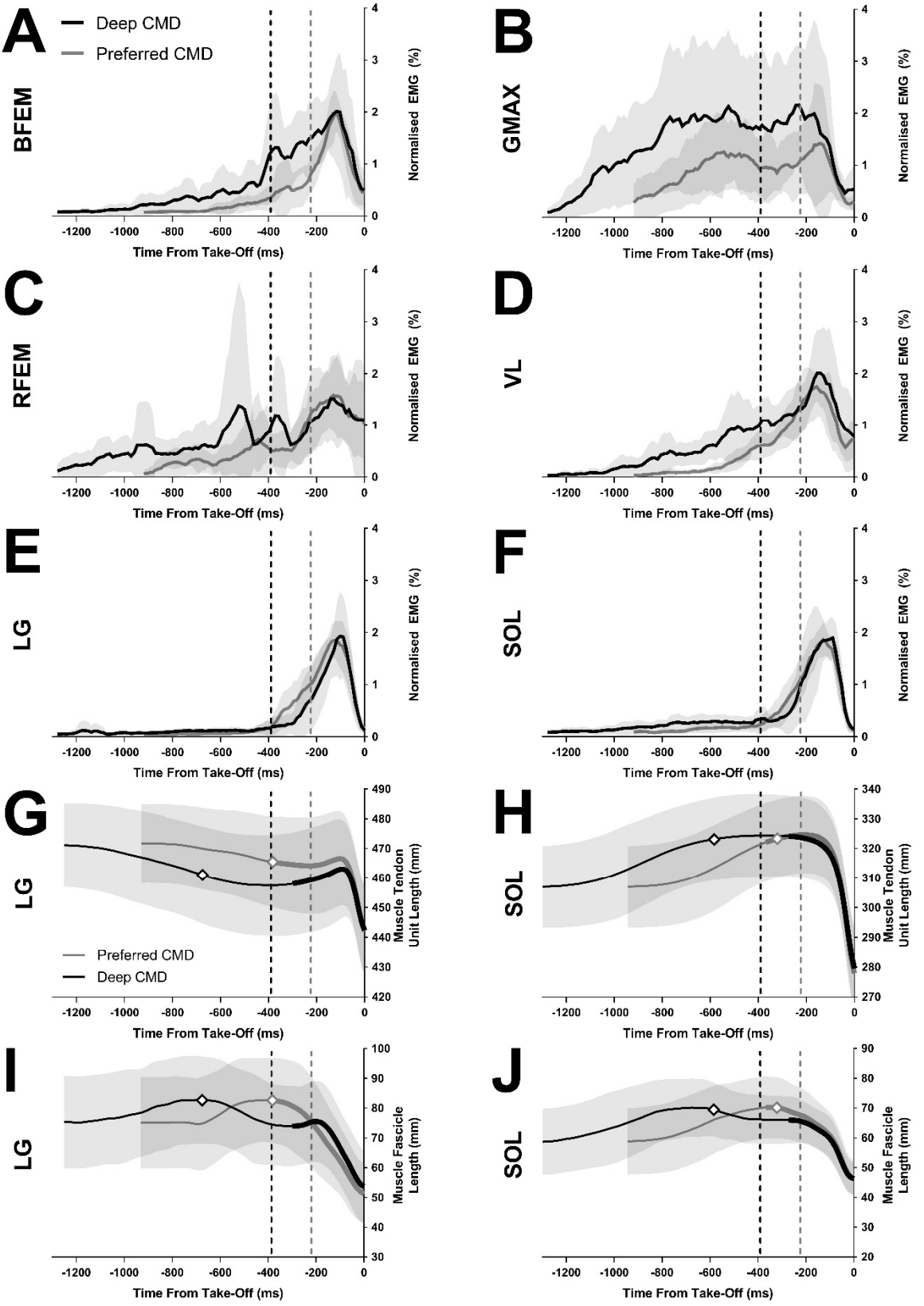

Figure 3: Mean (± STD) normalized EMG time series graphs of the BFEM (A), GMAX (B), RFEM (C), VL (D), LG (E) and SOL (F) muscles for the preferred and deep CMD conditions. Mean (± STD) MTU length (G & H) and muscle fascicle length (I & J) of the LG (G & I) and SOL (H & J) muscles. Time zero is the point of take-off. EMG was normalized to mean EMG during AFS of the preferred CMD condition. Diamonds indicate maximum fascicle length. Bold lines indicate AFS period. Vertical lines indicate the bottom of the countermovement. Maximal and integrated normalized EMG were compared using paired t-tests (N = 11). Muscle tendon unit and fascicle length change were compared using paired t-tests (N = 10).

Discussion

The aim of this study was to examine how muscle contractile mechanics and activation are altered to overcome a constrained task. As intended, total net work and jump height were not significantly different between conditions, while CMD was significantly deeper in the deep CMD condition. The hip demonstrated a greater range of motion, maximal moment and maximal activation (GMAX and BFEM) in the deep CMD compared to the preferred, facilitating a greater net joint work output. Net work at the ankle was significantly reduced in the deep CMD, primarily due to a reduced moment between conditions (ankle range of motion remained constant). Maximal EMG of the ankle plantar flexors was not significantly different between conditions and therefore the underlying muscle fascicle kinematics were implicated in reducing ankle joint work.

We hypothesized that necessary reductions in ankle work might be achieved in the deep CMD by active fascicle lengthening to reabsorb energy stored in the Achilles tendon ('backfire'). Tendon backfire was not exhibited as there was no evidence of active fascicle lengthening whilst the MTU shortened (Figure 3). Instead, we report a decreased ankle moment across the entire movement during the deep CMD condition (Figure 2), which suggests that less energy was stored in the Achilles tendon compared to the preferred CMD. This decrease in moment and work about the ankle in the deep CMD appears to be primarily due to a change in fascicle contraction timing, separating onset of fascicle shortening and substantial muscle activation in the LG (Figure 3), which resulted in reduced active fascicle length change and likely a less favorable operating position on the force-length relationship.

Due to the LG muscles' bi-articular nature, increased knee flexion resulted in a much shorter MTU length throughout most of the movement. LG fascicle length and length change during AFS were also reduced and was likely the primary contributor to the decrease in torque at the ankle (Figure 3G and I). SOL MTU length changes were not significantly different between conditions due to no change in ankle ROM and the SOL muscle's mono-articular nature. In the deep CMD, SOL fascicle length changes from the time of

342 maximal fascicle length until start of substantial muscle activation demonstrated a slight shortening and
343 then plateau, which coincided with a plateau in both the ankle angle and moment (Figure 2 and Figure 3).
344 Therefore, with reduced force production from the LG in the deep CMD, the SOL was potentially required
345 to produce a greater force in order to maintain ankle position and stability at the bottom of the
346 countermovement. During the deep CMD prior to substantial muscle activation, SOL muscle background
347 activation (Figure 3F) was slightly increased compared to the preferred CMD, therefore this small increase
348 in activation was potentially the cause for the slight shortening of SOL fascicle length with no difference in
349 MTU length (isometric contraction). As a result of early shortening in the deep CMD, SOL AFS was
350 reduced in the deep CMD compared to the preferred, albeit to a lesser degree than the LG. Previous studies
351 have demonstrated that increased knee flexion resulted in a significantly reduced moment about the ankle,
352 likely due to bi-articular gastrocnemius fascicles operating at very short lengths and neural inhibition down-
353 regulating force output at similar levels of central drive, resulting in decreased muscle activation (10, 23,
354 27). Maximal EMG between conditions was not significantly different in either the LG or SOL and
355 integrated EMG was only slightly decreased in the LG. Therefore, these results suggest that LG and SOL
356 muscle neural inputs remained fairly constant (Figure 3E and F) and as such, neural inhibition of the LG
357 from increased knee flexion was not likely a contributing factor to the decrease in force output. Thus, a
358 sub-optimal LG operating position on the force-length relationship and decreased AFS of the LG and SOL
359 might explain the reduction in ankle moment in the deep CMD compared to preferred.

360

361 Work and moments about the ankle were altered through changes in muscle contractile mechanics, which
362 served to limit the work output about the ankle (17, 49). Alternatively, the hip extensor muscles experienced
363 large changes in muscle activation timing to increase range of motion, hip joint moment and work output
364 (Figure 3A and B). This was due to hip extension occurring over a much greater period compared to ankle
365 plantar flexion and therefore more voluntary neural control adjustments may be employed. Bobbert et al.
366 (5) demonstrated similar shifts in muscle activation, with EMG onset of hip extensors and plantar flexors
367 separating during a deep CMD, although this was examined in SJ and only onset timing was examined.
368 Optimal feedback control theory suggests that human movement applies the best approximation of the
369 optimal solution based on the limitations of the task (46). Due to the short time interval over which plantar

370 flexion occurs (Figure 2C), feedback to inform changes in voluntary motor control (i.e. not a reflex) are
371 unlikely to be applied. The time taken to (i) process sensory information, (ii) produce a suitable motor
372 control pattern and (iii) activate the muscles is, at minimum, 100-130 ms using somatosensory feedback for
373 the fastest simple choice reaction movements (41). This is then delayed further by an additional lag (30-
374 50ms) between muscle activation and muscle force production (9). Therefore, movement adaptation during
375 plantar flexion will likely rely on resources with low (reflex) or no delay (muscle contractile mechanics).
376 While short and long-latency reflexes could potentially assist with joint coordination during ankle plantar
377 flexion (19, 42), the changes in muscle fascicle lengths suggest that changes in muscle contractile mechanics
378 are playing the primary role in adapting to this altered task constraint. Alternatively, if a muscle has a greater
379 movement time, then voluntary changes in activation strategy may be employed and used in conjunction
380 with low delay resources to alter muscle force production. Due to a proximal-to-distal joint coordination
381 strategy found in many tasks (6, 36, 39), distal muscles may be required to rely heavily on muscle contractile
382 properties to overcome constraints compared to proximal muscles. However, additional research of in vivo
383 proximal muscle mechanics is required to further explore this theory.

384

385 The results within this study also support the findings of Vanrenterghem el al. (54) who demonstrated that
386 humans perform submaximal jumping using strategies to minimize energy consumption. In addition to
387 having to overcome large inertial resistances of the proximal limbs, a deep CMD causes the bi-articular
388 gastrocnemius to perform work at unfavorably short lengths. Bi-articular muscles play a large role in transfer
389 of power from proximal muscles and fine tuning joint coordination (48, 51), therefore the bi-articular
390 gastrocnemius was likely still required to perform these roles even at unfavorably short lengths, although
391 potentially in a reduced capacity. Simulation studies have theorized that a deep CMD could produce a
392 greater maximal jump height, due to increased time to perform the movement facilitating a greater impulse,
393 however this has not been demonstrated in experimental data (12). The deep CMD in this paper had similar
394 or even more flexed knee angles than previous maximal jumping studies with a deep CMD (12, 45).
395 Therefore, during maximal jumping with a deep CMD, the bi-articular gastrocnemius muscle may be
396 shortened beyond optimal lengths, altering the muscle contractile mechanics and compromising the
397 potential for greater impulse to be achieved with a longer movement time.

The observed pattern of fascicle length change during the first half of the countermovement (start of movement to maximal fascicle length) differs from that presented by Kurokawa et al. (31), who suggested that the medial gastrocnemius fascicles remained isometric or shortened immediately after initiating the downward movement. The present study found a lengthening in the LG and SOL fascicles (Figure 3I and J), which is consistent with the required decrease in plantar flexor moment about the ankle to produce controlled dorsiflexion during the countermovement. The LG may not lengthen during this phase due to knee flexion counteracting ankle plantar flexion, however LG lengthening found in this study may be due to mechanical connections between the SOL and LG muscle bellies which would come under strain if the SOL lengthened to enable dorsiflexion without LG fascicle lengthening (4, 7, 32, 33, 37, 40).

Bi-articular muscles play an important role in fine tuning joint coordination and transferring energy from proximal-to-distal segments (47, 51, 58). The findings from this study further emphasize the vital role that bi-articular muscles play in movement coordination, especially at the ankle. Populations that suffer from motor impairment or amputees that are missing functional bi-articular muscles, may have impaired ability to fine-tune joint coordination. Further, most ankle prosthetics do not currently employ any feedback from knee motion to inform control of the prosthetic (1, 22). Therefore, such prosthetics may lack some of the inputs for control that the biological leg depends upon and designers should consider this in future devices.

Conclusion

This study examined muscle mechanics during submaximal countermovement jumping to understand how ankle muscle force and work output was regulated to obtain the target jump height. Changes in muscle kinematics that altered fascicle lengths and active fascicle shortening were observed as mechanisms for reducing plantar flexor force production. It may be that distal leg muscles which have very small activation periods rely on intrinsic properties to regulate force output in explosive movements, whereas proximal muscle activations are under more voluntary neural control.

Acknowledgements

Logan Wade was funded by an Australian Postgraduate Award. Dominic Farris and Glen Lichtwark did not receive any specific funding for this project. Logan Wade is currently supported by the Department for Health, University of Bath, Bath, BA2 7AY, United Kingdom.

Disclosures

None

Endnote

At the request of the authors, readers are herein alerted to the fact that additional materials related to this manuscript may be found at https://doi.org/10.24378/exe.1283. These materials are not a part of this manuscript and have not undergone peer review by the American Physiological Society (APS). APS and the journal editors take no responsibility for these materials, for the website address, or for any links to or from it. This material contains individual source data of time, moment, angle, EMG, muscle fascicle lengths and muscle tendon unit lengths for all joints and muscles analyzed within this manuscript, normalized to 101 points.

References

1. **Aldridge JM, Sturdy JT, and Wilken JM**. Stair ascent kinematics and kinetics with a powered lower leg system following transtibial amputation. *Gait & Posture* 36: 291-295, 2012.
2. **Aragón-Vargas LF**. Evaluation of Four Vertical Jump Tests: Methodology, Reliability, Validity, and Accuracy. *Measurement in Physical Education and Exercise Science* 4: 215-228, 2000.
3. **Astley HC, and Roberts TJ**. Evidence for a vertebrate catapult: elastic energy storage in the plantaris tendon during frog jumping. *Biology Letters* 2011.
4. **Bernabei M, Dieën JHv, Baan GC, and Maas H**. Significant mechanical interactions at physiological lengths and relative positions of rat plantar flexors. 118: 427-436, 2015.

5. **Bobbert MF, Casius LJR, Sijpkens IWT, and Jaspers RT**. Humans adjust control to initial squat depth in vertical squat jumping. *Journal of Applied Physiology* 105: 1428-1440, 2008.
6. **Bobbert MF, and Van Ingen Schenau GJ**. Coordination in vertical jumping. *Journal of Biomechanics* 21: 249-262, 1988.
7. **Bojsen-Møller J, Schwartz S, Kalliokoski KK, Finni T, and Magnusson SP**. Intermuscular force transmission between human plantarflexor muscles in vivo. *Journal of Applied Physiology* 109: 1608-1618, 2010.
8. **Cavagna GA, and Kaneko M**. Mechanical work and efficiency in level walking and running. *The Journal of Physiology* 268: 467-481, 1977.
9. **Cavanagh PR, and Komi PV**. Electromechanical delay in human skeletal muscle under concentric and eccentric contractions. *Europ J Appl Physiol* 42: 159-163, 1979.
10. **Cresswell AG, Löscher WN, and Thorstensson A**. Influence of gastrocnemius muscle length on triceps surae torque development and electromyographic activity in man. *Experimental Brain Research* 105: 283-290, 1995.
11. **Delp SL, Anderson FC, Arnold AS, Loan P, Habib A, John CT, Guendelman E, and Thelen DG**. OpenSim: Open-Source Software to Create and Analyze Dynamic Simulations of Movement. *IEEE Transactions on Biomedical Engineering* 54: 1940-1950, 2007.
12. **Domire ZJ, and Challis JH**. The influence of squat depth on maximal vertical jump performance. *Journal of Sports Sciences* 25: 193-200, 2007.
13. **Donelan JM, Kram R, and Arthur D. K**. Mechanical and metabolic determinants of the preferred step width in human walking. *Proceedings of the Royal Society of London Series B: Biological Sciences* 268: 1985-1992, 2001.
14. **Farris DJ, and Lichtwark GA**. UltraTrack: Software for semi-automated tracking of muscle fascicles in sequences of B-mode ultrasound images. *Computer Methods and Programs in Biomedicine* 128: 111-118, 2016.
15. **Farris DJ, Lichtwark GA, Brown NAT, and Cresswell AG**. The role of human ankle plantar flexor muscle-tendon interaction & architecture in maximal vertical jumping examined in vivo. *J Exp Biol* 219: 528-534, 2016.
16. **Farris DJ, and Raiteri BJ**. Elastic ankle muscle–tendon interactions are adjusted to produce acceleration during walking in humans. *The Journal of Experimental Biology* 220: 4252-4260, 2017.
17. **Gerritsen KGM, van den Bogert AJ, Hulliger M, and Zernicke RF**. Intrinsic Muscle Properties Facilitate Locomotor Control—A Computer Simulation Study. *Motor Control* 2: 206-220, 1998.
18. **Gordon AM, Huxley AF, and Julian FJ**. The variation in isometric tension with sarcomere length in vertebrate muscle fibres. *The Journal of Physiology* 184: 170-192, 1966.
19. **Gottlieb GL, and Agarwal GC**. Response to sudden torques about ankle in man: myotatic reflex. *Journal of Neurophysiology* 42: 91-106, 1979.
20. **Hamner SR, Seth A, and Delp SL**. Muscle contributions to propulsion and support during running. *Journal of Biomechanics* 43: 2709-2716, 2010.
21. **Hermens H, Freriks B, Merletti R, Stegeman D, Blok J, Rau G, Disselhorst-Klug C, and Hagg G**. *SENIAM 8*. Netherlands: Roessingh Research and Development, 1999.
22. **Herr HM, and Grabowski AM**. Bionic ankle–foot prosthesis normalizes walking gait for persons with leg amputation. *Proceedings of the Royal Society B: Biological Sciences* 279: 457-464, 2012.
23. **Herzog W, Read LJ, and ter Keurs HEDJ**. Experimental determination of force—length relations of intact human gastrocnemius muscles. *Clinical Biomechanics* 6: 230-238, 1991.
24. **Hill A**. The heat of shortening and the dynamic constants of muscle. *Proceedings of the Royal Society of London B: Biological Sciences* 126: 136-195, 1938.
25. **Hodges PW, and Bui BH**. A comparison of computer-based methods for the determination of onset of muscle contraction using electromyography. *Electroencephalography and Clinical Neurophysiology/Electromyography and Motor Control* 101: 511-519, 1996.

26. **Hogan N, Bizzi E, Mussa-Ivaldi FA, and Flash T**. Controlling multijoint motor behavior. *Exercise and sport sciences reviews* 15: 153-190, 1987.

27. **Kawakami Y, Ichinose Y, and Fukunaga T**. Architectural and functional features of human triceps surae muscles during contraction. *Journal of Applied Physiology* 85: 398-404, 1998.

28. **Kibele A**. Possibilities and limitations in the biomechanical analysis of countermovement jumps: A methodological study. *Journal of Applied Biomechanics* 14: 105-117, 1998.

29. **Kuo AD**. A Simple Model of Bipedal Walking Predicts the Preferred Speed–Step Length Relationship. *Journal of Biomechanical Engineering* 123: 264-269, 2001.

30. **Kurokawa S, Fukunaga T, and Fukashiro S**. Behavior of fascicles and tendinous structures of human gastrocnemius during vertical jumping. *Journal of Applied Physiology* 90: 1349-1358, 2001.

31. **Kurokawa S, Fukunaga T, Nagano A, and Fukashiro S**. Interaction between fascicles and tendinous structures during counter movement jumping investigated in vivo. *Journal of Applied Physiology* 95: 2306-2314, 2003.

32. **Maas H, Baan GC, and Huijing PA**. Intermuscular interaction via myofascial force transmission: effects of tibialis anterior and extensor hallucis longus length on force transmission from rat extensor digitorum longus muscle. *Journal of Biomechanics* 34: 927-940, 2001.

33. **Maas H, and Sandercock TG**. Force transmission between synergistic skeletal muscles through connective tissue linkages. *BioMed Research International* 2010: 2010.

34. **Mandic R, Jakovljevic S, and Jaric S**. Effects of countermovement depth on kinematic and kinetic patterns of maximum vertical jumps. *Journal of Electromyography and Kinesiology* 25: 265-272, 2015.

35. **Margaria R**. *Sulla fisiologia e specialmente sul consumo energetico della marcia e della corsa a varie velocita ed inclinazioni del terreno*. 1938.

36. **Marshall RN, and Elliott BC**. Long-axis rotation: The missing link in proximal-to-distal segmental sequencing. *Journal of Sports Sciences* 18: 247-254, 2000.

37. **Mehta R, Maas H, Gregor RJ, and Prilutsky BI**. Unexpected Fascicle Length Changes In Denervated Feline Soleus Muscle During Stance Phase Of Walking. *Scientific Reports* 5: 17619, 2015.

38. **Minetti AE, Ardigò LP, and Saibene F**. Mechanical determinants of the minimum energy cost of gradient running in humans. *The Journal of Experimental Biology* 195: 211-225, 1994.

39. **Novacheck TF**. The biomechanics of running. *Gait & Posture* 7: 77-95, 1998.

40. **Oda T, Kanehisa H, Chino K, Kurihara T, Nagayoshi T, Fukunaga T, and Kawakami Y**. In vivo behavior of muscle fascicles and tendinous tissues of human gastrocnemius and soleus muscles during twitch contraction. *Journal of Electromyography and Kinesiology* 17: 587-595, 2007.

41. **Pascual-Leone A, Brasil-Neto JP, Valls-Solé J, Cohen LG, and Hallett M**. Simple reaction time to focal transcranial magnetic stimulation: Comparison with reaction time to acoustic, visual and somatosensory stimuli. *Brain* 115: 109-122, 1992.

42. **Pruszynski JA, and Scott SHJEBR**. Optimal feedback control and the long-latency stretch response. 218: 341-359, 2012.

43. **Richards CT, and Sawicki GS**. Elastic recoil can either amplify or attenuate muscle–tendon power, depending on inertial vs. fluid dynamic loading. *Journal of Theoretical Biology* 313: 68-78, 2012.

44. **Roberts TJ, and Azizi E**. The series-elastic shock absorber: tendons attenuate muscle power during eccentric actions. *Journal of Applied Physiology* 109: 396-404, 2010.

45. **Salles AS, Baltzopoulos V, and Rittweger J**. Differential effects of countermovement magnitude and volitional effort on vertical jumping. *Eur J Appl Physiol* 111: 441-448, 2011.

46. **Todorov E, and Jordan MI**. Optimal feedback control as a theory of motor coordination. *Nature Neuroscience* 5: 1226, 2002.

47. **van Ingen Schenau G, Bobbert M, and van Soest A**. The Unique Action of Bi-Articular Muscles in Leg Extensions. In: *Multiple Muscle Systems*, edited by Winters J, and Woo S-YSpringer New York, 1990, p. 639-652.
48. **Van Ingen Schenau GJ, Bobbert MF, and Rozendal RH**. The unique action of bi-articular muscles in complex movements. *Journal of Anatomy* 155: 1-5, 1987.
49. **van Soest A, and Bobbert M**. The contribution of muscle properties in the control of explosive movements. *Biol Cybern* 69: 195-204, 1993.
50. **Van Soest AJ, Bobbert MF, and Van Ingen Schenau GJ**. A control strategy for the execution of explosive movements from varying starting positions. *Journal of Neurophysiology* 71: 1390-1402, 1994.
51. **van Soest AJ, Schwab AL, Bobbert MF, and van Ingen Schenau GJ**. The influence of the biarticularity of the gastrocnemius muscle on vertical-jumping achievement. *Journal of Biomechanics* 26: 1-8, 1993.
52. **Vanrenterghem J, Bobbert MF, Casius LJR, and De Clercq D**. Is energy expenditure taken into account in human sub-maximal jumping? - A simulation study. *Journal of Electromyography and Kinesiology* 18: 108-115, 2008.
53. **Vanrenterghem J, De Clercq D, and Van Cleven P**. Necessary precautions in measuring correct vertical jumping height by means of force plate measurements. *Ergonomics* 44: 814-818, 2001.
54. **Vanrenterghem J, Lees A, Lenoir M, Aerts P, and De Clercq D**. Performing the vertical jump: Movement adaptations for submaximal jumping. *Human Movement Science* 22: 713-727, 2004.
55. **Wade L, Lichtwark G, and Farris DJ**. Movement Strategies for Countermovement Jumping are Potentially Influenced by Elastic Energy Stored and Released from Tendons. *Scientific Reports* 8: 2300, 2018.
56. **Wade L, Lichtwark GA, and Farris DJ**. The influence of added mass on muscle activation and contractile mechanics during submaximal and maximal countermovement jumping in humans. *The Journal of Experimental Biology* 222: jeb194852, 2019.
57. **Werkhausen A, Albracht K, Cronin NJ, Meier R, Bojsen-Møller J, and Seynnes OR**. Modulation of muscle–tendon interaction in the human triceps surae during an energy dissipation task. *The Journal of Experimental Biology* 220: 4141-4149, 2017.
58. **Zajac FE**. Muscle coordination of movement: A perspective. *Journal of Biomechanics* 26, Supplement 1: 109-124, 1993.

Figure Legends

Figure 1: Net work about the hip (white), knee (grey) and ankle (black) joints during the preferred and deep countermovement depth conditions. Joint work was compared using a two-way repeat measures ANOVA (N = 12).

Figure 2: Mean (± STD) joint angles (A, B and C) and moments (D, E and F) about the hip (A and D), knee (B and E) and ankle (C and F) during the preferred CMD (Grey) and the deep CMD (Black). Vertical lines indication bottom of the countermovement. Joint range of motion and peak moment were analyzed (N = 12) using a two-way repeat measures ANOVA.

Figure 3: Mean (± STD) normalized EMG time series graphs of the BFEM (A), GMAX (B), RFEM (C), VL (D), LG (E) and SOL (F) muscles for the preferred and deep CMD conditions. Mean (± STD) MTU length (G & H) and muscle fascicle length (I & J) of the LG (G & I) and SOL (H & J) muscles. Time zero is the point of take-off. EMG was normalized to mean EMG during AFS of the preferred CMD condition. Diamonds indicate maximum fascicle length. Bold lines indicate AFS period. Vertical lines indicate the bottom of the countermovement. Maximal and integrated normalized EMG were compared using paired t-tests (N = 11). Muscle tendon unit and fascicle length change were compared using paired t-tests (N = 10).